Allosterism and Cooperativity in *Pseudomonas aeruginosa* GDP-Mannose Dehydrogenase†

Laura E. Naught, Sunny Gilbert, Rebecca Imhoff, Christopher Snook, Lesa Beamer, and Peter Tipton*

Department of Biochemistry, University of Missouri, Columbia, Missouri 65211

Received March 25, 2002; Revised Manuscript Received May 7, 2002

ABSTRACT: GDP-Mannose dehydrogenase catalyzes the formation of GDP-mannuronic acid, which is the monomeric unit from which the polysaccharide alginate is formed. Alginate is secreted by the pathogenic bacterium *Pseudomonas aeruginosa* and is believed to play an important role in the bacteria's resistance to antibiotics and the host immune response. We have characterized the kinetic behavior of GDP-mannose dehydrogenase in detail. The enzyme displays cooperative behavior with respect to NAD^+ binding, and phosphate and GMP act as allosteric effectors. Binding of the allosteric effectors causes the Hill coefficient for NAD^+ binding to decrease from 6 to 1, decreases $K_{1/2}$ for NAD^+ by a factor of 10, and decreases V_{max} by a factor of 2. The cooperative binding of NAD^+ is also sensitive to pH; deprotonation of two residues with identical p*K*'s of 8.0 is required for maximally cooperative behavior. The kinetic behavior of GDP-mannose dehydrogenase suggests that it must be at least hexameric under turnover conditions; however, dynamic light-scattering measurements do not provide a clear determination of the size of the active enzyme complex.

Alginate is a polysaccharide that is produced by the human pathogenic bacterium *Pseudomonas aeruginosa*. The bacteria secrete alginate to generate a capsule that is believed to serve a protective role against antibiotics and host immune responses. In addition, alginate is a primary constituent of the biofilm, the organized community that the bacteria develop upon colonization of host tissue (*1*). Bacteria living in biofilms typically have greatly reduced susceptibility to antibiotics compared to when they exist in their planktonic form (*2*).

Alginate is a linear copolymer of partially acetylated β-mannuronic acid residues and α-guluronic acid residues. The precursor to alginate is a homopolymer of β-mannuronic acid residues, and GDP-mannuronic acid serves as the biosynthetic donor of mannuronic acid units for the growing polysaccharide. GDP-mannuronic acid is the product of the reaction catalyzed by GDP-mannose dehydrogenase, an NAD^+-dependent enzyme that catalyzes the four-electron oxidation of the C6 hydroxyl group of GDP-mannose to the corresponding acid. Alginate biosynthesis in *P. aeruginosa* has been reviewed (*3*).

GMD[1] is encoded by the *algD* gene in *P. aeruginosa* and was reported to be a hexamer of 48 kDa subunits (*4*). Most of the genes encoding the enzymes responsible for alginate biosynthesis are organized into an operon; *algD* is the first gene in the operon and its promoter controls the expression of the other genes in the operon as well. The substrate specificity of GMD and some of its kinetic properties have been reported. The purified enzyme shows susceptibility to inactivation by thiol-reactive reagents, and mutation of a putative active site cysteine, C268, to serine was reported to reduce activity by 95% (*3*). The participation of cysteine in the catalytic reaction is reminiscent of glyceraldehyde 3-phosphate dehydrogenase in which a thiohemiacetal species is a key intermediate, although it is surprising that so much residual activity remains in the mutant GMD. Elegant studies of the related enzyme UDP-glucose dehydrogenase have suggested that its reaction also proceeds via a thiohemiacetal intermediate (*5*). It is proposed that the nucleotide-sugar dehydrogenases catalyze the NAD^+-dependent oxidation of the substrate C6 hydroxyl group to an aldehyde; addition of the cysteine side chain to the aldehyde forms the thiohemiacetal intermediate, and oxidation by a second equivalent of NAD^+ generates an acyl-enzyme species whose hydrolysis leads to the observed product. An analogous mechanism was long believed to be operative for histinol dehydrogenase, but mutational analysis of the conserved cysteines revealed that none were essential for catalytic activity (*6*).

We report here detailed kinetic studies of GMD as a prelude to mechanistic studies and efforts to prepare inhibitors or inactivators. We have found that GMD exhibits complex kinetic behavior; significant cooperativity was observed under some conditions, and GMP was found to function as an allosteric effector.

MATERIALS AND METHODS

All biochemicals were obtained from Sigma and were used without further purification.

The *algD* gene was amplified from *P. aeruginosa* PAO1 using primers that were designed based on the published sequence (*7*). *Nde*I and *BamH*I restriction sites were incor-

† Supported by NIH Grant GM59653.

* To whom correspondence should be addressed. Phone: (573) 882-7968, Fax: (573) 884-4812. E-mail: tiptonp@missouri.edu.

[1] Abbreviations: GMD, GDP-mannose dehydrogenase; IPTG, isopropyl β-D-1-thiogalactopyranoside; PMSF, phenylmethanesulfonyl fluoride; TLCK, *N*-α-*p*-tosyl-L-lysine chloromethyl ketone; DTT, dithiothreitol; DNAD, deamidoNAD.

10.1021/bi025862m CCC: $22.00
Published on Web 07/04/2002

porated into the primers so that the amplicon could be cloned into the pET-3a vector (Novagen) for expression. For production of GMD BL21(DE3), cells were transformed with the expression vector and grown in shake flasks in 6 L batches in LB medium containing 100 μg/mL ampicillin. Cells were grown at 37 °C until they reached an optical density of 0.6−0.8 at 600 nm, when expression was induced by the addition of IPTG to a final concentration of 0.4 mM. The cells were allowed to grow 4−5 h longer and were harvested by centrifugation. The cell paste was stored at −80 °C until use.

Purification of GMD. The purification of GMD followed the published protocol, with minor changes. Frozen cells were thawed in 50 mM Tris acetate (pH 7.6), containing 1 mM DTT, 2 mM $MgSO_4$, and 2 mM $CaCl_2$; 1 mL of buffer per gram of cell paste was used. TLCK and PMSF were each added to a final concentration of 0.5 mM. The cells were lysed by the addition of 0.2 mg/gram of cell paste of lysozyme and 10 μg/mL of DNase I. The solution was incubated with gentle shaking at 37 °C for 1 h and sonicated briefly. All subsequent manipulations were performed on ice or in a cold box at 4 °C. The cell debris was separated by centrifugation and discarded. Protamine sulfate was added dropwise to the supernatant from a stock solution prepared in water. The total amount of protamine sulfate added equaled 3 mg/gram of cell paste. The precipitated nucleic acids were removed by centrifugation, and the resulting crude extract was purified by acid fractionation and heat treatment as described (*4*). GMD from the heat treatment step was incubated with DNase I and RNase A, to digest contaminating nucleic acids that remained in the preparation. The nucleic acids were separated from the protein either with a desalting column (BioRad Bio-Gel P-6 DG) or a gel filtration column (Pharmacia Superdex 200, 1.8 × 80 cm) equilibrated in 50 mM Tris acetate (pH 7.6), containing 1 mM DTT, 100 mM NaCl, and 10% (w/v) glycerol.

An alternative purification was devised in order to avoid the acid fractionation and heat treatment steps in the original purification. The crude extract was treated with protamine sulfate as described previously and then fractionated with ammonium sulfate; GMD activity precipitated between 45% saturation and 60% saturation. Precipitated GMD was collected by centrifugation, dissolved in a small volume of buffer, treated with DNase I and RNaseA, and chromatographed on a Superdex 200 column as described previously.

GMD Assay. GMD activity was determined by monitoring the formation of NADH spectrophotometrically. The standard assay solution contained 0.1 mM GDP-mannose, 1.0 mM NAD^+, 1 mM DTT, and 7.5% (w/v) glycerol in 50 mM potassium phosphate (pH 8.0). Other conditions that were used are described in the text; all assays were conducted in buffer containing 7.5% (w/v) glycerol. Initial velocity kinetic studies were performed by monitoring NADH production by either absorbance or fluorescence spectroscopy in cuvettes maintained at 25 °C with a circulating water bath. Absorbance measurements were conducted with a Hewlett-Packard 8452A diode array spectrophotometer or a Cary 50 spectrophotometer; fluorescence measurements were conducted with an SLM Aminco 8100 spectrofluorometer. Kinetic data obtained by fluorescence measurements were in arbitrary units (fluorescence units per second); however, when absolute velocities were required, the rate data were converted to units of micromoles per second using a calibration curve constructed with known concentrations of NADH, measured at the same instrument settings as were used in the kinetics experiments.

Dynamic Light-Scattering Measurements. The hydrodynamic radius of GMD was measured by dynamic light-scattering using a Protein Solutions DynaPro 99/MSTC200 instrument with Dynamics v5.26.38 software. The protein concentration in all of the samples was 0.36 mg/mL; measurements were conducted at 20 ± 0.1 °C in buffers containing 7.5% (w/v) glycerol.

Data Analysis. Single substrate variation initial velocity patterns showing hyperbolic kinetics were fitted to the Michaelis−Menten equation, and those showing sigmoidal kinetics were fitted to the Hill equation (eq 1).

$$v = VA^n/(K + A^n) \quad (1)$$

Kinetic data obtained when both substrates were varied were fitted to eq 2, which describes sequential binding of substrates A and B.

$$v = VAB/(K_{ia}K_b + K_aB + K_bA + AB) \quad (2)$$

Inhibition data were fitted to eqs 3−5 for competitive, uncompetitive, and noncompetitive inhibition, respectively.

$$v = VA/[K(1 + I/K_{is}) + A] \quad (3)$$

$$v = VA/[K + A(1 + I/K_{ii})] \quad (4)$$

$$v = VA/[K(1 + I/K_{is}) + A(1+ I/K_{ii})] \quad (5)$$

Kinetic parameters from the pH variation studies were fitted to eq 6, which describes a wave-shaped pH profile, and to eq 7, which describes a pH profile with a limiting slope of 1 on the acid side and a limiting slope of −2 on the basic side, where the two basic p*K*'s are identical. In eqs 6 and 7, *Y* is the kinetic parameter being fitted and *C* is the pH-independent value of *Y*.

$$Y = \frac{\lim_1 + \lim_2 10^{(pK-pH)}}{1 + 10^{(pK-pH)}} \quad (6)$$

$$Y = \frac{C}{1 + 10^{(pK_1- pH)} + 10^{(pH-pK_2)} + 10^{2(pH-pK_2)}} \quad (7)$$

The Hill coefficients for the reaction in Tris buffer determined as a function of pH were fitted to eq 8, where n_{lo} and n_{hi} are the limiting values for the Hill coefficient at low and high pH, respectively.

$$n_{obs} = \frac{n_{lo}}{1 + 10^{2(pH-pK)}} + \frac{n_{hi}}{1 + 10^{2(pK-pH)}} \quad (8)$$

The apparent K_m's for NAD^+ as a function of the allosteric effector concentration were fitted to eq 9, where K_{app} is the measured K_m at a given effector concentration, *X* is effector concentration, $K_a°$ is the K_m for NAD^+ in the absence of effector, $K_x°$ is the dissociation constant for effector in the absence of NAD^+, and *Q* is the coupling parameter describing the interrelationship between binding of effector and NAD^+. The apparent values of V_{max} as a function of effector

Table 1: Dead-End Inhibition of the GMD Reaction

varied substrate	fixed substrate	inhibitor	K_{is} (μM)	K_{ii} (mM)	inhibition pattern
GDP-mannose	NAD (200 μM)	GMP	12.6 ± 1.0		C
NAD	GDP-mannose (15 μM)	GMP	14.1 ± 2.5	19.3 ± 3.4	NC
NAD	GDP-mannose (15 μM)	DNAD	112 ± 28	50.8 ± 4.5	NC
GDP-mannose	NAD (200 μM)	DNAD		28.6 ± 2.8	UC

concentration were fitted to eq 10, where V_{app} is the measured value of

$$K_{app} = K_a^\circ\left(\frac{K_x^\circ + X}{K_x^\circ + QX}\right) \quad (9)$$

$$V_{app} = V^\circ\left(\frac{K_x^\circ + QWX}{K_x^\circ + QX}\right) \quad (10)$$

V_{max} at a given effector concentration, V° is V_{max} in the absence of effector, K_x° and Q are as previously defined, and W is the ratio of V_{max} at infinite effector to V_{max} at zero effector.

RESULTS

Cloning, Overexpression, and Purification of GMD. The *algD* gene obtained by PCR amplification of *P. aeruginosa* PAO1 DNA matched the published sequence with very minor differences. Two silent mutations were noted, and codon 359, which was reported to be TTC, coding for phenylalanine, was TTG in our clone, coding for leucine, which matched the sequence obtained in the *Pseudomonas* genome sequencing project (*8*). Subcloning *algD* into the pET-3a vector and expressing it in *Escherichia coli* BL21(DE3) cells resulted in high level production of GMD. The published protocol for purification of GMD proved to be satisfactory; in fact, the HPLC gel filtration column used in the original purification was not found to be necessary. GMD that was greater than 90% homogeneous based on Coomassie Blue staining of SDS polyacrylamide gels was routinely obtained; this material proved satisfactory for crystallization.[2] However, it was observed that the GMD preparations were contaminated with nucleic acids; brief digestion with DNase and RNase followed by desalting or gel filtration was sufficient to remove the nucleic acids. GMD that was purified by ammonium sulfate fractionation and gel filtration chromatography did not differ in activity or purity from the enzyme purified using the acid fractionation and heat treatment steps.

Kinetic Mechanism. The kinetic mechanism of GMD was determined in potassium phosphate buffer at pH 8.0 using standard methodologies for multisubstrate enzymes (*9*). Michaelis−Menten kinetic behavior was observed in all experiments conducted in phosphate buffer. The reciprocal plot of initial velocities obtained with GDP-mannose as the variable substrate and NAD^+ as the changing fixed substrate showed a family of intersecting lines. The K_m for GDP-mannose was 4.1 ± 0.7 μM and the K_m for NAD^+ was 92 ± 10 μM. The results of dead-end inhibition studies using DNAD and GMP are summarized in Table 1, and the reciprocal plots for inhibition by GMP are shown in Figure 1.

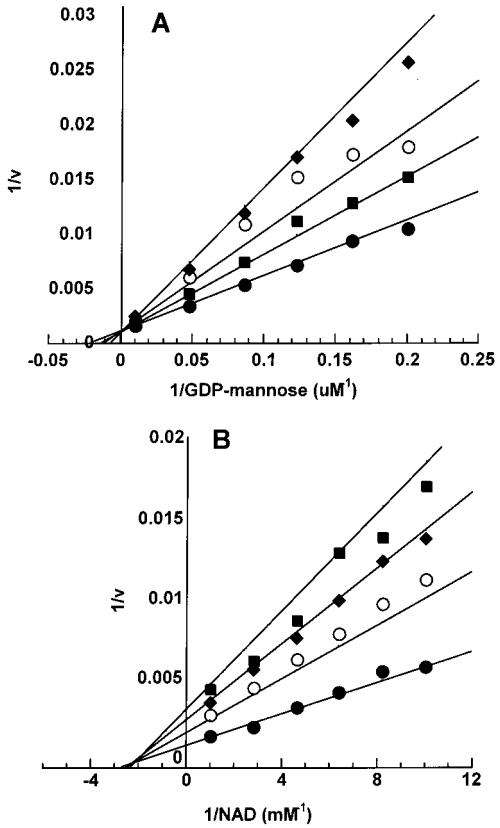

FIGURE 1: Reciprocal plots for inhibition of GMD by GMP. (A) Inhibition versus GDP-mannose. GMP concentrations were 0 (●), 5 (■), 10 (○), and 20 μM (◆). The points are experimental and the lines are the fit to eq 3. (B) Inhibition versus NAD. GMP concentrations were 0 (●), 10 (○), 20 (◆), and 30 μM (■). The points are experimental and the lines are the fit to eq 5.

Non-Michaelis−Menten Behavior. The kinetic behavior of GMD was markedly influenced by reaction conditions, protein concentration, and even order of addition of reaction components (Figure 2). In Tris buffer at pH 8.0, reactions initiated by the addition of GMD to solutions containing all of the substrates exhibited a significant burst of product formation and then slowed dramatically. Reactions initiated by the addition of either GDP-mannose or NAD^+ to solutions containing GMD and the other reaction components did not exhibit a burst, and the initial velocity approximated the velocity observed after the burst phase in the reactions initiated by addition of enzyme. When the reaction was conducted in phosphate buffer at pH 8.0, there was no burst and no order of addition effect was observed; similarly, when the reaction was conducted in Tris (pH 8.0) in the presence of 100 μM GMP (vide infra), there was no burst and no order of addition effect.

For those reactions conducted in Tris at pH 8.0 and initiated by addition of GMD, plots of the velocity of the burst phase versus NAD^+ concentration were sigmoidal; however, the degree of the cooperativity, turnover number,

[2] Snook, C. Unpublished observations.

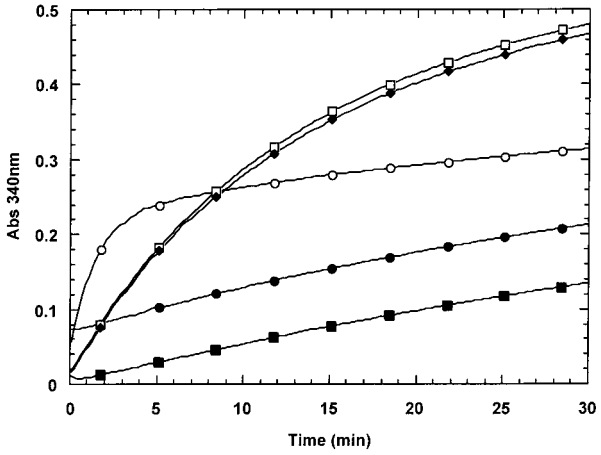

FIGURE 2: GMD reaction time courses. All reactions were conducted at pH 8.0 at a GMD concentration of 0.01 mg/mL. Final GDP-mannose concentration was 50 μM; final NAD^+ concentration was 1 mM. Reaction in Tris, initiated by addition of GMD (○); reaction in Tris, initiated by addition of NAD^+ (●); reaction in Tris, initiated by addition of GDP-mannose (■); reaction in Tris in the presence of 100 μM GMP, initiated by addition of GMD (□); reaction in potassium phosphate, initiated by addition of GMD (◆).

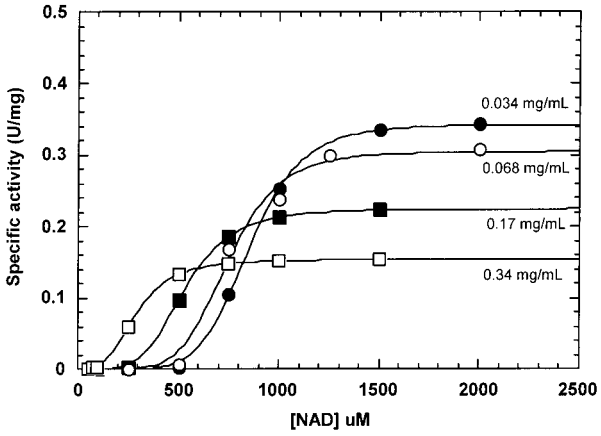

FIGURE 3: Protein concentration dependence of the GMD reaction. Final GMD concentrations in the cuvette were 0.34 (□), 0.17 (■), 0.068 (○), and 0.034 mg/mL (●). The points are experimental and the lines are the fits to eq 1.

and $K_{1/2}$ for NAD^+ were functions of the GMD concentration. This is illustrated in Figure 3 where the velocities obtained at different enzyme concentrations are represented in units of μmol/min/mg GMD. It can be seen that increasing concentrations of GMD diminish the cooperativity, decrease $K_{1/2}$ for NAD^+, and decrease the turnover number.

GMD Effectors. Addition of phosphate to Tris buffer at pH 8.0 affected the cooperativity, as reflected in the Hill coefficient, as well as $K_{1/2}$ for NAD^+ and V_{max} (Figure 4A). The effect of phosphate on $K_{1/2}$ and V_{max} was evaluated quantitatively using the linked-function formalism (*10*) (Figure 4B); fitting the $K_{1/2}$ data to eq 9 yielded a value for the coupling parameter Q of 5.9 ± 0.6. $K_x°$ the dissociation constant for NAD^+ from GMD in the absence of P_i was 970 ± 25 μM, and the dissociation constant for P_i in the absence of NAD^+ was 15 ± 3 mM. K_x^∞, the dissociation constant for NAD from GMD at saturating P_i, can be calculated as $K_x^\infty = K_x°/Q$, yielding a value of 160 μM. Apparent values of V_{max} measured at different P_i concentrations were fitted to eq 10; the fit was performed utilizing the values of Q and $K_x°$ determined from the analysis of the $K_{1/2}$ data as fixed parameters. The fit yielded a value for W, the ratio of the limiting values of V_{max} in the presence and absence of P_i, of 0.34 ± 0.02 (i.e., the reaction was 3 times slower in the presence of saturating P_i than in its absence).

The Hill coefficient decreased with increasing P_i (Figure 4C). It should be noted that data obtained at high P_i concentrations and fitted to the Hill equation yielded values for the Hill coefficient >1; however, satisfactory fits to the Michaelis−Menten equation (i.e., Hill coefficient equal to 1) could also be obtained.

One of the effects of P_i is to stimulate GMD activity at low NAD^+ concentration, even though the activity is lower at high NAD^+ concentration. A series of potential effectors was screened for compounds that could similarly stimulate GMD activity in Tris buffer. The enzyme was incubated with 50 μM NAD^+ and 100 μM GDP-mannose in Tris buffer; in the absence of effectors, reaction was essentially undetectable under these conditions. The following compounds were tested at a concentration of 100 μM: malate, fumarate, citrate, succinate, α-ketoglutarate, mannose 1-P, mannose 6-P, GTP, GDP, GMP, and AMP. Coenzyme A was tested at 10 μM, and KCl was tested at 50 mM. The only compound that stimulated the GMD reaction was GMP; the velocity of the reaction in the presence of 100 μM GMP was increased up to a level that was 31% of the velocity of the reaction in phosphate buffer alone.

The effect of GMP was investigated in detail (Figure 5). Like P_i, the effect of GMP was to decrease V_{max}, $K_{1/2}$ for NAD^+, and the Hill coefficient. Fitting the $K_{1/2}$ data to eq 9 yielded a value of 3.7 ± 0.3 for Q; $K_{1/2}$ for NAD^+ in the absence of GMP was 950 ± 5 μM, in good agreement with the value determined in the P_i variation experiments, and the dissociation constant for GMP was 94 ± 15 μM. The calculated values of $K_x°$ and Q yield a value of 250 μM for K_x^∞, the dissociation constant for NAD^+ from the GMD−GMP complex. Attempts to fit the V_{max} data to eq 10 failed to converge; the reason is apparent from inspection of Figure 5B. The V_{max} data do not reach a stable plateau value at high GMP concentrations; rather, V_{max} continues to decrease with increasing GMP concentration. The Hill coefficient is quite sensitive to the presence of GMP (Figure 5C) and plateaus at a value of 1 at 100 μM GMP.

pH Effects. The pH dependence of the kinetic parameters of the GMD reaction in potassium phosphate buffer was determined in the pH range from 6.5 to 8.2 (Figure 6). The V/K profile revealed the presence of two or three ionizable groups, one on the acid limb of the bell-shaped curve and one or two on the basic limb of the curve. The data were best fitted by a function describing three ionizations (eq 7), but they can also be described adequately by a function describing only one ionization on the acid limb and one ionization on the basic limb of the pH profile, and it is possible that the superior fit to eq 7 is fortuitous. The pK's were not separated sufficiently such that their values could be determined (the fit provides the value of the sum of the pK's, but cannot distinguish their individual values). The V_{max} profile was wave-shaped with higher values of V_{max} at high pH; the pK defined by the transition from one plateau to the other was 7.3 ± 0.2.

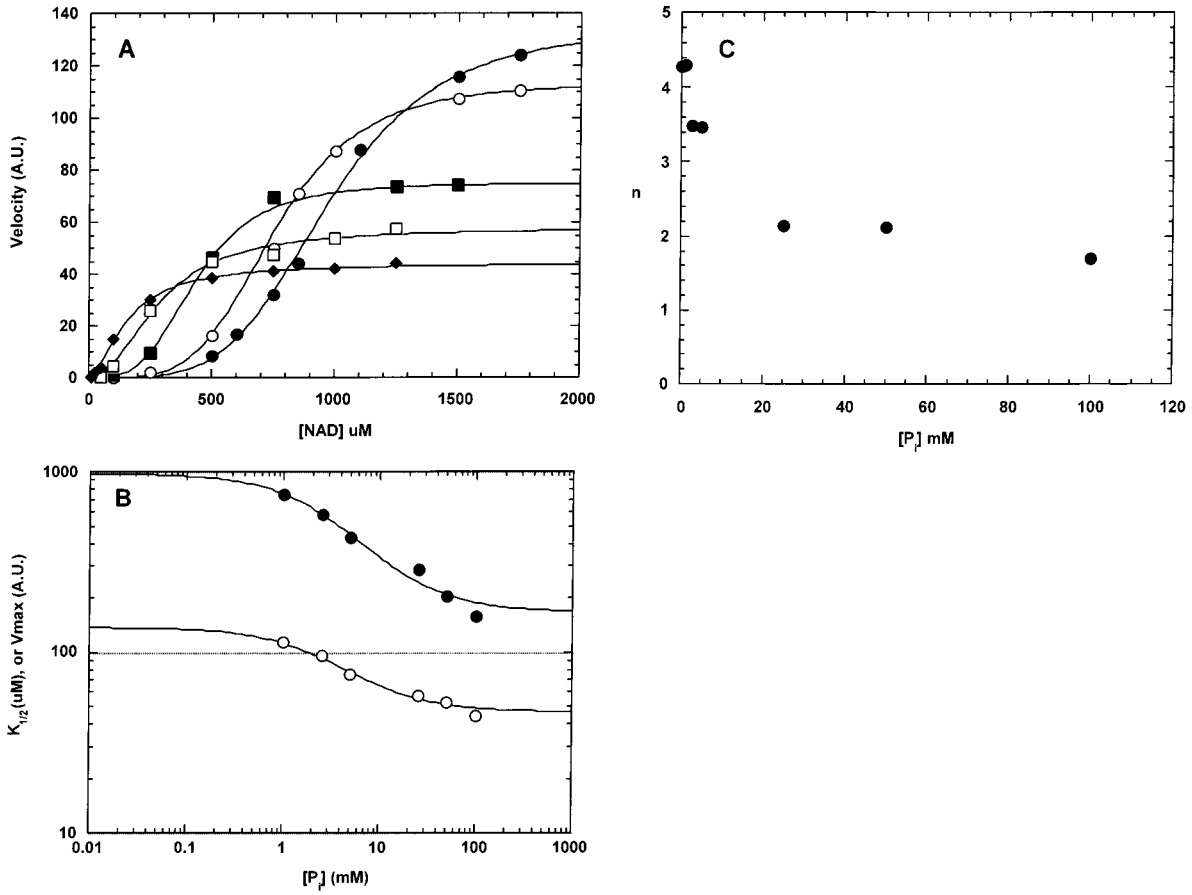

FIGURE 4: Effect of P_i on the GMD reaction. (A) Reaction velocity in the presence of P_i. Velocities are in arbitrary units. P_i concentrations were 0 (●), 1 (○), 5 (■), 25 (□), and 100 mM (◆). The individual traces were fitted to eq 1. (B) $K_{1/2}$ (●) for NAD^+ and V_{max} (○) as a function of P_i concentration. The points are experimental; the line through the $K_{1/2}$ data is the fit to eq 9, and the line through the V_{max} data is the fit to eq 10. (C) The Hill coefficient as a function of P_i concentration.

The pH dependence of the reaction in Tris buffer was also monitored. The Hill coefficient was extremely sensitive to pH, decreasing from a plateau value of 6.2 ± 0.3 at high pH to a value of 0.8 ± 0.2 at low pH (Figure 7). The data were fitted to eq 8, which assumes that ionization of two residues with the same p*K* occurs in the transition between the high and low plateaus; the fit yielded a value for the p*K*'s of 8.00 ± 0.05. Fitting the data to a function that assumes ionization of only one residue resulted in a significantly poorer fit.

Dynamic Light-Scattering Measurements. The translational diffusion coefficient of GMD was measured under different solution conditions, and the data were used to calculate its hydrodynamic radius and apparent molecular weight (Table 2). The molecular weight of the GMD subunit, calculated from the amino acid sequence deduced from the *algD* nucleotide sequence, is 47.4 kDa. Under most of the conditions tested, the calculated GMD molecular weights defined a broad distribution centered approximately around the value expected for a trimer; in the presence of 200 mM NaCl or in 50 mM triethanloamine acetate, GMD appeared hexameric but polydisperse. The standard deviation of the hydrodynamic radius for each sample is indicated in Table 2 and can be taken as a quantitative measure of the polydispersity of the sample; values less than 30% of the measured hydrodynamic radius are considered to be monomodal (*11*). The baseline in all of the measurements was 1.000 ± 0.003.

DISCUSSION

GMD catalyzes the committed step in alginate biosynthesis and a detailed understanding of its catalytic properties should aid efforts to design inhibitors that may be useful for attenuating alginate production in bacterial infections. Because alginate is believed to contribute to the ability of *P. aeruginosa* to resist antibiotic therapies, the development of such inhibitors may be clinically useful.

The kinetic behavior of GMD proved to be considerably more complex than initial studies had indicated to be the case. The sensitivity of GMD to reaction conditions was remarkable. In phosphate buffer, GMD exhibited Michaelis−Menten kinetics, but in Tris, it displayed marked cooperativity with respect to NAD^+ binding. Closer investigation revealed that phosphate is an allosteric effector of GMD and that GMP was identified as another allosteric effector. No cooperativity with respect to GDP-mannose binding was observed under any of the conditions tested. The maximum value observed for the Hill coefficient for NAD^+ was around 6, which is the maximal value expected for a hexameric enzyme. The maximal velocity that was achieved in Tris was about twice that in phosphate buffer; the concentration of NAD^+ required to achieve half-maximal velocity in Tris was around 1 mM. In contrast, the K_m for NAD^+ in phosphate buffer was about 0.1 mM.

To begin to characterize the kinetic behavior of GMD in more detail, we utilized the fact that GMD displays Michaelis−Menten kinetics in phosphate buffer, so the order of

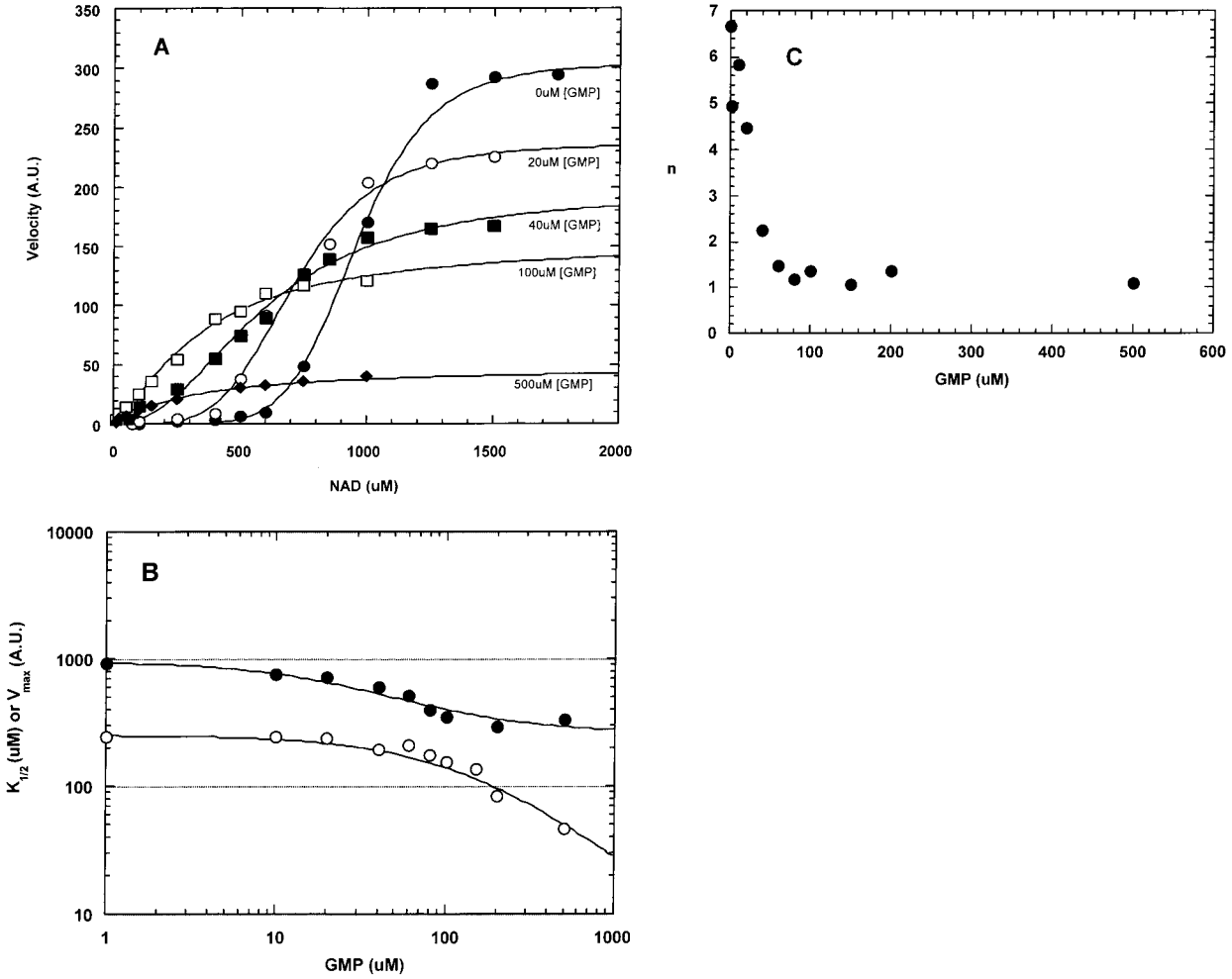

FIGURE 5: Effect of GMP on the GMD reaction. (A) Reaction velocity in the presence of GMP. Velocities are in arbitrary units. GMP concentrations were 0 (●), 20 (○), 40 (■), 100 (□), and 500 μM (◆). The individual traces were fitted to eq 1. (B) $K_{1/2}$ (●) for NAD^+ and V_{max} (○) as a function of GMP concentration; the points are experimental. The $K_{1/2}$ data were fitted to eq 9; the V_{max} data did not converge to a fit to eq 10, and the line is drawn to guide the eye. (C) The Hill coefficient as a function of GMP concentration.

Scheme 1

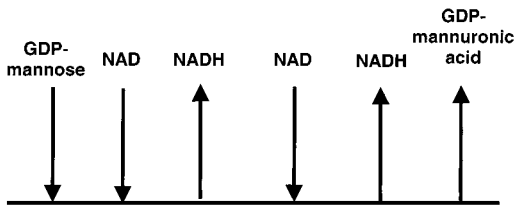

substrate binding and product release and the pH dependence of the kinetic parameters could be studied using standard approaches. The catalytic reaction consumes 2 equiv of NAD^+ and 1 equiv of GDP-mannose and produces GDP-mannuronic acid and 2 equiv of NADH. Dead-end inhibitors were used rather than product inhibitors because GDP-mannuronic acid is not commercially available and NADH, the other product, could not be used in high concentrations in the fluorescence assay used in these experiments. Results from initial velocity kinetic studies are summarized in Table 1 and are fully consistent with what is formally a bi uni uni bi ping-pong mechanism (Scheme 1). Note that parallel patterns are not observed in initial velocity experiments because, although the addition points of the second and third substrates are separated by an irreversible step, both substrates are NAD^+. The dead-end inhibitor GMP is competitive versus GDP-mannose, indicating that they bind to the

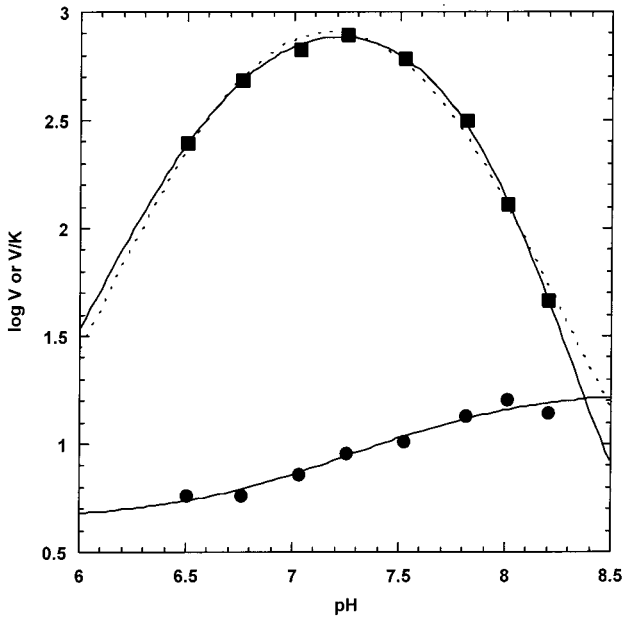

FIGURE 6: pH dependence of $(V/K)_{NAD}$ (■) and V_{max} (●) in phosphate buffer. The V/K data were fitted to eq 7 ($\chi^2 = 0.0012$), and the V_{max} data were fitted to eq 6. The dashed line shows the fit of the V/K data to a function with a single ionization on the acid side and a single ionization on the basic side ($\chi^2 = 0.015$).

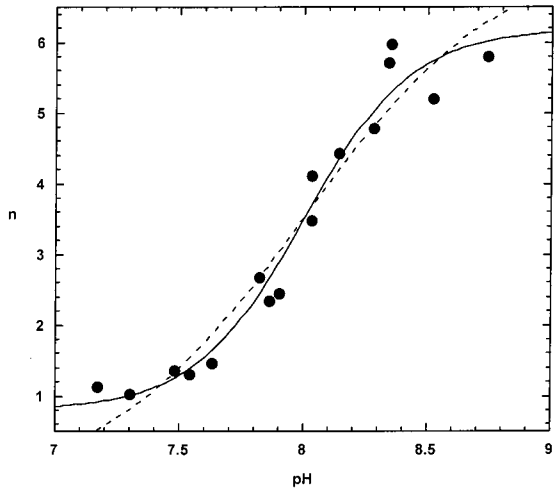

FIGURE 7: pH dependence of the Hill coefficient for the GMD reaction in Tris buffer. The points are experimental and the line is the fit to eq 8 ($\chi^2 = 1.73$). The dashed line is the fit to eq 6 ($\chi^2 = 3.23$).

same enzyme form. GMP inhibition is noncompetitive versus NAD^+, so these results suggest that GMP adds to an enzyme form that is upstream of the form to which NAD^+ adds, that is, free enzyme. Consistent with these results is the uncompetitive inhibition displayed by DNAD versus GDP-mannose; uncompetitive inhibition indicates that the inhibitor adds to the enzyme downstream of the point where the substrate added. It is perhaps counterintuitive that DNAD does not display competitive inhibition versus NAD; however, the fact that NAD^+ binds to two different forms of the enzyme, the enzyme−GDP-mannose binary complex and the enzyme−aldehyde intermediate complex, accounts for the presence of both slope effects and intercept effects in the inhibition pattern.

It is formally possible that GMD contains distinct binding sites for each molecule of NAD^+ that is required in the reaction. However, the sequence contains only one recognizable nucleotide-binding motif, from residues 2−19 (*12*), and the crystal structure of the related enzyme UDP-glucose dehydrogenase from *Streptococcus pyogenes* shows a single NAD(H) binding site (*13*). Therefore, a ping-pong mechanism in which one NAD^+ binds, undergoes reduction, dissociates from the enzyme, and is replaced by a second NAD^+ in the same binding site seems likely.

The cooperativity that is observed in Tris buffer presumably reflects the addition of NAD^+ to the enzyme−GDP-mannose−effector ternary complex. This conclusion is based on the determination of the ordered kinetic mechanism in phosphate buffer. However, further experimentation will be required to determine whether GMD follows the same kinetic mechanism in Tris; the observation that preincubation of GMD with either NAD^+ or GDP-mannose affects the kinetic behavior of the enzyme (Figure 1) implies that either substrate can bind to free enzyme. Nonetheless, even if GMD adopts a random kinetic mechanism in Tris buffer, the cooperativity experiments were conducted using saturating concentrations of GDP-mannose, so the enzyme−GDP-mannose−effector complex should be the predominant complex in solution to which NAD^+ adds.

The cooperative kinetic behavior that was observed implies that GMD functions as a multisubunit enzyme. Indeed, GMD was reported to elute from a gel filtration column as a hexamer (*4*). We investigated the quaternary structure of GMD by dynamic light scattering, which provides a measure of the hydrodynamic radius of the protein from which the apparent molecular weight can be calculated. As shown in Table 2, GMD did behave approximately as expected for a hexamer in triethanolamine buffer and in phosphate buffer containing 0.2 M NaCl, which were used in the gel filtration chromatography reported by Roychoudhury et al. However, GMD showed only modest cooperativity under these conditions, characterized by a Hill coefficient of about 2. The fact that addition of 0.2 M NaCl to phosphate buffer serves to favor formation of a high molecular weight complex suggests that hydrophobic interactions promote multimer formation. In both instances where high molecular weight GMD complexes were observed, the samples were polydisperse. The dynamic light-scattering measurements in the absence of triethanolamine or NaCl yielded values for the molecular weight of GMD that were considerably smaller than expected for a hexamer. Furthermore, the calculated molecular weight values varied widely, and these results are difficult to reconcile with the kinetic data.

The value of 6 for the Hill coefficient implies that GMD is at least hexameric under the conditions of the kinetic assays; however, the dynamic light-scattering measurements provided no evidence for hexamer formation under conditions where maximal cooperativity is observed. It is important to note that the light-scattering measurements were conducted using relatively high concentrations of GMD and that maximal cooperativity was observed at lower concentrations of protein and decreased with increasing protein concentration (Figure 3). We were unable to obtain satisfactory light-scattering data at the low protein concentrations where Hill coefficients of 6 were observed, and it is not attractive to suggest that more subunit association should be observed at lower protein concentrations.

Taken at face value, the dynamic light-scattering measurements suggest that GMD is trimeric under most solution conditions, and one can imagine hexamer formation occurring via transient dimerization of trimers. However, if dimerization were a part of the catalytic cycle, the velocity of the reaction should be proportional to the square of the enzyme concentration, and that is not observed (data not shown). Clearly, the relationship between the quaternary structure of GMD and its cooperative behavior requires further examination. It is important to emphasize that a Hill coefficient of 6 implies that a hexameric enzyme is the smallest enzyme complex that could easily accommodate the kinetic data; larger enzyme complexes with less dramatic cooperativity could give rise to the observed kinetic data as well.

The pH dependence of the Hill coefficient is suggestive of some protein−protein interaction with a stoichiometry of 2 being required for maximal cooperativity. The Hill coefficient varies in a pH-dependent manner from 6 above pH 8 to 1 at pH 7; the data describing the transition between the plateaus fit well to a function in which ionization of two residues with identical p*K*'s dictates the distribution between the cooperative and noncooperative forms of GMD. This behavior could be accommodated by a model in which corresponding residues on two subunits must deprotonate to form the complex that displays cooperative behavior.

The GMD hexamer that appeared to form in triethanolamine and high ionic strength buffer must be different from

Table 2: Dynamic Light-Scattering Measurements of GMD

sample[a]	buffer	$R_h \pm$ std dev (nm)	MW (kDa)
GMD	KP, pH 7.0	5.55 ± 1.64	185
GMD	KP, pH 8.0	4.82 ± 0.45	131
GMD	Tris, pH 7.0	4.92 ± 0.33	138
GMD	Tris, pH 8.0	4.68 ± 0.83	122
GMD, GMP[b]	Tris, pH 8.0	5.38 ± 1.02	171
GMD, DNAD,[b] GDP-mannose[b]	KP, pH 8.0	5.44 ± 0.74	176
GMD, DNAD, GDP-mannose	Tris, pH 8.0	5.26 ± 0.61	163
GMD, NAD, GDP-mannose[c]	KP, pH 8.0	5.43 ± 0.73	175
GMD[d]	KP, pH 7.0 0.2 M NaCl	6.87 ± 2.42	307
GMD[d]	TEA acetate, pH 7.6	7.11 ± 2.89	337

[a] Except where indicated, samples included 7.5% (w/v) glycerol. [b] When included in the sample, GMP was present at 500 μM, DNAD at 1 mM, and GDP-mannose at 100 μM. [c] GDP-mannose, 10 mM; NAD, 20 mM. [d] Data obtained in the absence of glycerol.

the enzyme complex observed under other turnover conditions because it did not display cooperativity. The fact that the turnover number of the enzyme decreases when the protein concentration in the assay solution is increased also suggests that oligomerization can occur to form complexes different from those formed under optimal turnover conditions.

Although P_i acted as an allosteric effector for GMD, the concentrations at which its effects were manifested were quite high, so it seemed likely that P_i was acting as a surrogate for a more physiologically significant effector. Thus, we sought to determine whether any other allosteric effectors could be found. GMD was assayed in the presence of 50 μM NAD^+, which is insufficient to support significant turnover when the enzyme behaves cooperatively but which supports considerable activity when the enzyme follows Michaelis−Menten kinetics, as in phosphate buffer. KCl at 50 mM was without effect, demonstrating that the effect in potassium phosphate buffer was due to phosphate and not potassium. A series of metabolites that are substrates or products of the alginate pathway was examined, and GMP was observed to stimulate the activity of GMD significantly. Other guanosine nucleotides and metabolites that are found in the alginate pathway were examined as well, but did not stimulate GMD.

Control of alginate production and energy metabolism via the Krebs cycle have been shown earlier to be coordinated through the action of the protein encoded at the *algR2* locus. Alginate production requires AlgR2 (*14*); it was also observed that an *algR2*(-) strain of *P. aeruginosa* had decreased levels of phosphorylated succinyl CoA synthetase and nucleoside diphosphate kinase (*15*). In *P. aeruginosa*, these two enzymes are isolated as a complex; GDP is a substrate for succinyl CoA synthetase, and the GTP produced in its reaction is used as the substrate to phosphorylate ADP in the reaction catalyzed by nucleoside diphosphate kinase. It has been pointed out that energy metabolism and alginate production must be tightly coordinated in mucoid *P. aeruginosa* (*15*), because up to 50% of the carbon source available to the bacteria can be diverted to alginate synthesis (*16*). Our observation that the activity of GDP-mannose dehydrogenase is regulated by GMP indicates that alginate production should be sensitive to GMP levels and suggests that the relative levels of the GMP, GDP, and GTP may be a critical determinant for growth and alginate production in mucoid *P. aeruginosa*. AlgR2 has no effect on Krebs cycle enzymes other than succinyl CoA synthetase (*15*), and no Krebs cycle intermediates that we tested had any effect on the activity of GMD.

The influence of GMP on the kinetic behavior of GMD was examined in terms of the linked-function formalism (*10*). Figure 5 shows that GMP decreases the K_m for NAD^+, V_{max}, and the Hill coefficient for GMD. The free energy of interaction between GMP and NAD^+ can be calculated from the relationship $\Delta G = -RT \ln Q$, so the measured value for Q of 3.7 indicates that binding of NAD^+ to the GDP-mannose−GMD−GMP complex is 0.8 kcal/mol more favorable than binding to the binary complex in the absence of GMP.

It should be noted that these experiments were conducted in the presence of saturating GDP-mannose, which implies that GDP-mannose and GMP can bind to the enzyme simultaneously. However, sequence analysis does not reveal an obvious second nucleotide binding site on GMD. It is possible that the GMP binding site is composed of residues from different subunits and so does not form until the enzyme adopts a specific quaternary structure. This model provides a facile role for the allosteric effector; to stabilize one quaternary form of the enzyme versus another.

Equation 9 assumes that binding of GMP to the enzyme occurs without cooperativity; however, one can see that the data points define a steeper transition between the high K_m and low K_m plateaus than the fit to the equation, suggesting that GMP binding is, in fact, cooperative.

The V_{max} data could not be fitted to a linked-function equation because they did not reach a stable minimum value (Figure 5B). Examination of Figure 5C, which shows the apparent Hill coefficient as a function of GMP concentration, suggests a possible explanation. As GMP increases from 0 to 100 μM, the Hill coefficient rapidly decreases to 1. Thus, GMD behaves noncooperatively at GMP concentrations above 100 μM. At low concentrations of GMP, V_{max} is invariant, suggesting that GMP acts primarily as a K-type allosteric effector with regard to NAD^+ binding. Above 100 μM, GMP V_{max} begins to decrease, and there is no indication in the data that it would level off before 0. This behavior presumably arises through binding of GMP at the GDP-mannose site. Because V_{app} is a function of the available active sites, it decreases as the active sites become filled with GMP. On the other hand, GMP is a noncompetitive inhibitor versus NAD^+ and the apparent K_m for NAD^+ is almost independent of the GMP concentration (the lines in the reciprocal plot cross near the abcissa; Figure 1), and eq 9

can be utilized for evaluating the binding of NAD^+ as a function of GMP concentration.

The derivation of the kinetic mechanism of GMD based on the interpretation of the GMP inhibition data in phosphate buffer should be valid, because the experiments were conducted under conditions where the allosteric site would be filled with P_i. The reactions were conducted in 50 mM phosphate buffer, 3 times the dissociation constant for P_i from GMD, and the highest concentration of GMP used in the inhibition studies was 30 μM, less than one-third of the value of its dissociation constant from the allosteric site.

Although GMD has much lower affinity for phosphate than for GMP, phosphate is not a potent competitive inhibitor versus GDP-mannose; thus, its effect on K_m and V_{max} can be evaluated more clearly. The linked-function analysis of the GMD reaction in Tris buffer in the presence of varying amounts of phosphate is shown in Figure 4. As with GMP, phosphate binding to GMD lowers the K_m for NAD^+, in this case by a factor of 10. V_{max} is also decreased in the presence of increasing phosphate concentration; however, the effect on V_{max} is only 3-fold, not nearly as substantial as the effect on K_m. Qualitatively, P_i and GMP have the same effect on GMD, and they behave primarily as K-type allosteric effectors.

Thus, the data suggest that GMD interconverts readily between two forms, the "cooperative" form that is stabilized in Tris buffer and which binds NAD^+ with relatively low affinity and which has a higher V_{max} and a "noncooperative" form that is stabilized by phosphate or GMP binding and which has much greater affinity for NAD^+ but a lower V_{max}. To our knowledge, allosteric behavior has not been noted previously for GMD. After the GMP allosteric sites have been filled, GMP appears to compete with GDP-mannose for binding to the active site; as GDP-mannose becomes displaced from the enzyme, V_{max} decreases accordingly. In the noncooperative form of the enzyme, GMP binding and GDP-mannose binding is mutually exclusive, because a competitive inhibition pattern is observed.

The pH dependence of the kinetic parameters in phosphate buffer reveals that several critical ionizations occur within the limited pH range where phosphate buffer can be utilized. The V_{max} profile is wave-shaped; protonation of a species with a pK of 7.3 causes a 4-fold decrease in V_{max}. Wave-shaped pH profiles arise when the enzyme can adopt two states that differ with respect to protonation but which are both competent to catalyze the reaction. The pK that is defined by the V_{max} profile in the GMD reaction matches the pK of phosphate; it is quite possible that the wave-shaped pH profile arises because GMD has different affinities for the phosphate monoanion and phosphate dianion and, thus, that the distribution between the P_i-bound form of GMD and the P_i-free form of GMD shifts with pH. If this is indeed the case, because the P_i-bound form of GMD exhibits a lower V_{max}, the data suggest that it predominates below pH 7.3; in other words, GMD binds the phosphate monoanion more tightly than the phosphate dianion.

The $(V/K)_{NAD}$ pH profile shows two or three ionizations, one or two of which do not appear in the V_{max} profile and, therefore, must arise from groups that must be in the correct protonation state for catalysis to occur. The roles of these residues are not known at present, but the participation of a general base to abstract a proton from the hydroxyl group undergoing oxidation is expected. General acid catalysis would be expected to facilitate formation of the tetrahedral species that must form from the aldehyde before the second oxidation takes place. If a thiohemiacetal species is an intermediate in the reaction, general acid and base catalysis would be expected to facilitate its hydrolysis.

GMD is an attractive target for inhibition because it has no analogue in humans and it catalyzes the committed step in alginate biosynthesis. Characterization of potential inhibitors requires that the kinetic behavior of the target enzyme be well-defined; the studies presented here demonstrate that the functional behavior of GMD is quite sensitive to the conditions used in in vitro studies and provide a framework with which to evaluate inhibitors. Furthermore, the observation that GMP is an allosteric effector of GMD provides another mechanism by which alginate production and energy metabolism may be linked in *P. aeruginosa*.

ACKNOWLEDGMENT

We are grateful to Dr. Jennifer Kimmel for many helpful discussions.

REFERENCES

1. Hentzer, M., Teitzel, G. M., Balzer, G. J., Heydorn, A., Molin, S., Givskov, M., and Parsek, M. R. (2001) *J. Bacteriol. 183* (18), 5395−5401.
2. Nickel, J. C., Ruseska, I., Wright, J. B., and Costerton, J. W. (1985) *Antimicrob. Agents Chemother. 27* (4), 619−624.
3. Shankar, S., Ye, R. W., Schlictman, D., and Chakrabarty, A. M. (1995) *Adv. Enzymol. Relat. Areas Mol. Biol. 70*, 221−255.
4. Roychoudhury, S., May, T. B., Gill, J. F., Singh, S. K., Feingold, D. S., and Chakrabarty, A. M. (1989) *J. Biol. Chem. 264* (16), 9380−9385.
5. Ge, X., Campbell, R. E., van de Rijn, I., and Tanner, M. E. (1998) *J. Am. Chem. Soc. 120*, 6613−6614.
6. Teng, H., Segura, E., and Grubmeyer, C. (1993) *J. Biol. Chem. 268* (19), 14182−14188.
7. Deretic, V., Gill, J. F., and Chakrabarty, A. M. (1987) *Nucleic Acids Res. 15* (11), 4567−4581.
8. Stover, C. K., Pham, X. Q., Erwin, A. L., Mizoguchi, S. D., Warrener, P., Hickey, M. J., Brinkman, F. S., Hufnagle, W. O., Kowalik, D. J., Lagrou, M., Garber, R. L., Goltry, L., Tolentino, E., Westbrock-Wadman, S., Yuan, Y., Brody, L. L., Coulter, S. N., Folger, K. R., Kas, A., Larbig, K., Lim, R., Smith, K., Spencer, D., Wong, G. K., Wu, Z., and Paulsen, I. T. (2000) *Nature 406* (6799), 959−964.
9. Cleland, W. W. (1970) in *The Enzymes* (Boyer, P. D., Ed.) 3rd ed., Vol. 2, pp 1−65, Academic Press, New York.
10. Reinhart, G. D. (1983) *Arch. Biochem. Biophys. 224* (1), 389−401.
11. Biswas, I., Ban, C., Fleming, K. G., Qin, J., Lary, J. W., Yphantis, D. A., Yang, W., and Hsieh, P. (1999) *J. Biol. Chem. 274* (33), 23673−23678.
12. Dougherty, B. A., and van de Rijn, I. (1993) *J. Biol. Chem. 268* (10), 7118−7124.
13. Campbell, R. E., Mosimann, S. C., van De Rijn, I., Tanner, M. E., and Strynadka, N. C. (2000) *Biochemistry 39* (23), 7012−7023.
14. Deretic, V., and Konyecsni, W. M. (1989) *J. Bacteriol. 171* (7), 3680−3688.
15. Schlictman, D., Kavanaugh-Black, A., Shankar, S., and Chakrabarty, A. M. (1994) *J. Bacteriol. 176* (19), 6023−6029.
16. Mian, F. A., Jarman, T. R., and Righelato, R. C. (1978) *J. Bacteriol. 134* (2), 418−422.

BI025862M